APPLICATION OF A MULTIDISCIPLINARY APPROACH TO ASSESS CONSOLIDATION IN DIFFERENT GEOLOGICAL LAYERS AT A LOCAL SCALE IN ANTWERP

Atefe Choopani[1,2], Philippe Orban[2], Pierre-Yves Declercq[1], Xavier Devleeschouwer[1], Alain Dassargues[2]

[1] Royal Belgium Institute of Natural Sciences, Geological Survey of Belgium, Rue Jenner 13, 1000 Brussels,

[2] Liège University, Hydrogeology & Environmental Geology, Urban & Environmental Engineering, allée de la Découverte 9, 4000 Liège

ABSTRACT

Antwerp region in Belgium is suffering land subsidence at least since 1948 owing to a combination of human and natural factors. Before the current study, the spatial extent and magnitude of this subsidence had been detected and measured using the Persistent Scatterer Interferometry (PSI) technique. A 3D-finite-difference groundwater flow model using MODFLOW coupled to a 1D-geomechanical model (named SUB - Subsidence and aquifer system compaction) of 1 square kilometer located within the area where subsidence is observed. It was developed to estimate the consolidation that occurred over time in the different hydrogeological layers. Simulation results consist of time series of vertical deformation in the 9 layers of the model over 2007-2016. The total simulated displacements were compared to PSI surface measurements from ENVISAT data processed between 2007-2010. The simulated and observed values are fairly in agreement in the considered zone.

Index Terms— SUB package, PSI, MODFLOW, groundwater flow, consolidation, subsidence

1. INTRODUCTION

Numerous research focused on the identification and monitoring of ground displacement using various geodetic techniques, particularly the Persistent Scatterer Interferometry (PSI) approach [1]. Based on these monitoring results, effort must be continued for determining the intricate mechanisms that are responsible for surface displacement. In Antwerp, a subsidence bowl is identified, mapped, and measured by the processing of ERS1/2 (1992-2001), ENVISAT (2003-2010), and Sentinel-1A (2016-2019) through the PS-InSAR algorithm [2]. In this study, a 1D-geomechanical model is used to compute the elastic and inelastic displacements in various sub-layers at the local scale over 2007-2016. Piezometric data that monitor the water level in the local zone is only available during this period. The Envisat PSI data were used to validate the results of 1D-geomechanical simulation for the years 2007 to 2010.

2. STUDY AREA

Due to its lowland topography, the harbour city of Antwerp, which is located on low-lying floodplains in the upper part of the Sea Scheldt estuary, has historically experienced periodic flooding. A dike was constructed around the city to control inundation and flow patterns. Additionally, excavated debris was used to cover a 106 km² area with embankments. Along the dikes, this backfill varies in thickness from 1.2 to 8.2 meters. Indeed, the additional stress imposed by the embankment weight has probably induced additional subsidence as observed by the PSI technique in the whole area. Here, we decided to investigate the other causes of subsidence mainly linked to pore pressure variations in the different underground layers. So, to exclude this impact of the embankment load, we decided to study an area of 1 km² chosen outside the embankment close to the southwestern border (Fig. 1).

3. DATA AND MEASUREMENTS

3.1. Hydrogeological data

Nine hydrogeological units, comprising four aquifers (layers 2, 4, 6, 8), four aquitards (layers 3, 5, 7, 9), and one aquitard/aquifer are identified as forming the shallow aquifer system (i.e., aquifers and confining layers) up to a depth of 225 m. From top to bottom, the successive geological formations are: sand and clay polder deposits (Formation of Flanders - HCOV[1] 0130), sand of aeolian overburden, and clayey sand Pliocene aquifer system (Formation of Ghent, Lillo, and Powderlee – HCOV 0150 to 0220), clayey sands of Kattendijk, Kasterlee and Boom clay (Formation of Kattendijk, Kasterlee, and Boom – HCOV 0240 and 0300), sandy Ruisbroek-Berg aquifer (upper

[1] HCOV is Hydrogeologische Codering van de Ondergrond van Vlaanderen (Dutch name of the hydrogeological coding system within the geological database system of Flanders).

Zelzate Formation – HCOV 0430), Tongeren clay aquitard (middle Zelzate Formation – HCOV 0440), sandy Lower Oligocene Aquifer System (lower Zelzate Formation – HCOV 0450), Bartoon clay Aquitard (Formation of Maldegem – HCOV 0500), Wemmel-Lede Aquifer and sands of Brussels (Formation of Lede, Aalter, upper Gentbrugge – HCOV 0600) and Paniselian clay Aquitard System (lower Gentbrugge Formation – HCOV 0700).

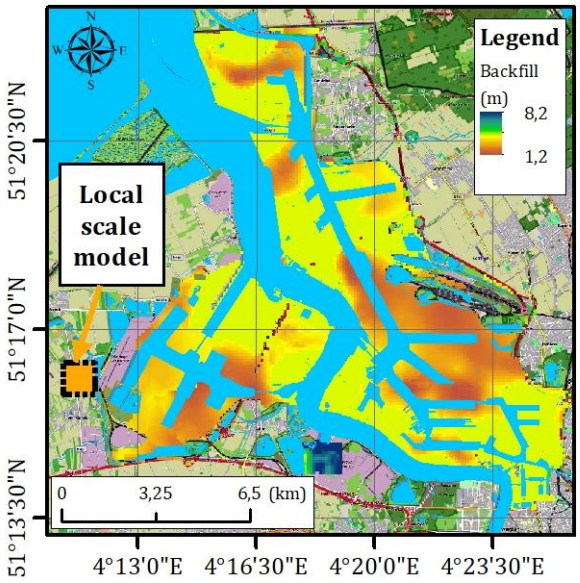

Figure 1: Location of the study area situated on the southwestern border of the backfill of the Antwerp harbor.

The evolution of groundwater levels (i.e., piezometric heads) between 2007-2016 in the different aquifers was prescribed to the eastern and western sides of the model using observations in 3 piezometric monitoring wells. Through two separate screens, a piezometric well located on the western border was measuring piezometric heads in both aquifers 4 and 8. The piezometric head evolution in the second aquifer was provided by a second piezometric well on the eastern side. The third piezometer was located at a 3.7 kilometers distance from the western side. To be as realistic as possible, the piezometric time evolution measured in the closest monitoring wells is projected on the associated model boundary in accordance with the observed gradient in the only piezometric map that is currently available (i.e., dating of the fall of 2009). The northern and southern boundaries of the aquifer layers and all boundaries of low permeable layers were considered as no-flow boundaries.

Hydrogeological parameters including horizontal and vertical hydraulic conductivity values were collected from the reports of previous studies about regional groundwater modeling in various parts of Flanders [3]. Hydrogeological parameters defined in the flow model are indicated in Table 1. A regular grid is chosen in the XY horizontal planes with cell dimensions of 100 m. Along the Z axis, each cell has a variable dimension depending on the bottom and top elevation of the associated layer. The Subsurface Databank of Flanders was used to gather information on the top and bottom heights of each layer.

Layer	HCOV code	$K_h(m/s)$	$K_v(m/s)$
Layer 1	130	1.50E-05	3.00E-06
Layer 2	0150-0220	1.17E-04	2.62E-05
Layer 3	0240+0300	1.30E-11	4.00E-11
Layer 4	0430	4.50E-05	1.13E-05
Layer 5	0440	1.16E-09	1.65E-10
Layer 6	0450	2.85E-05	2.85E-07
Layer 7	0500	2.61E-11	4.82E-11
Layer 8	600	1.61E-04	4.01E-05
Layer 9	0700	2.50E-12	5.00E-13

Table 1: Values of vertical and horizontal hydraulic conductivity parameters in different layers

3.2. Geomechanical data

Although the relationship between effective stress (ln σ') and deformation is typically nonlinear, it is possible to linearize the relationship with regards to the preconsolidation effective stress (σ'_{max}) when using two separate parameters for 'skeletal specific storage' of the saturated porous medium (S_{sk}), one for stresses higher than the preconsolidation stress (inelastic deformation) and the other for stresses lower (elastic deformation).

Four major geomechanical parameters that can be measured by oedometer tests (i.e., 1D drained consolidation tests) and under the hypothesis of linear stress-strain relation are compression constant (C), swelling constant (A), compression index (C_C), and swelling index (C_S) [4,5]. These parameters allow computing the compressibility in both elastic and inelastic conditions. Therefore, two separate parameters for the 'skeletal specific storage' coefficient under elastic and inelastic conditions will be estimated (S_{ske} and S_{skv}). To simulate the displacement time series of each layer, these two parameters are the most critical needed data.

Four samples, all taken from boreholes on the western side of the boundary, were used to gather the geomechanical parameters for shallower geological units in the local model of Antwerp [6]. No samples were found within or close to the border for Boom clay or deeper layers. The values of the geomechanical parameters were collected from samples taken from the Kallo, Essen, and Mol sites located respectively at distances of 7, 29, and 72 km from the center of the local model [7,8].

3.3. Subsidence data

From the PSI analysis of ERS1/2, ENVISAT, and Sentinel-1A radar data, ground movement measurements at the

location of Permanent Scatterers (PS) points in the whole of Antwerp harbour are provided for the time periods 1992–2001, 2003–2010, and 2016–2022, respectively [2]. 6, 18, and 25 PS points are detected during the time span of ERS1/2, ENVISAT, and Sentinel-1A, respectively, inside the boundary of local models.

Between all PSs within the local model boundary, the average subsidence velocity along the Line Of Sight (LOS) of the satellite has been estimated to be -1.5, -1.1, and -2.4 mm/year for the three periods, respectively.

4. 1D-GEOMECHANICAL COUPLED TO 3D-FLOW MODEL

Due to groundwater exploitation, pore pressure changes (as induced by piezometric head changes) are inducing effective stress changes in the 1D model column. This hydromechanical coupling is the cause of the deformation observed at the land surface [9]. Any decrease of pore pressure is translated in an equivalent increase of effective stress. The pore pressure propagation in the different layers is very rapid in aquifers but can be delayed in low permeability layers. With no or delayed drainage, the SUB module of MODFLOW allows to simulate both elastic (recoverable) and inelastic (non-recoverable) interbed compactions [10]. In fact, for a slight change in effective stress ($\Delta\sigma'/\sigma' \rightarrow 0$) and assuming all deformation induced by the head change, the deformation of the layer can be approximately calculated as follow:

$$\Delta b = S_{sk} b \Delta h \quad (1)$$

$$S_{sk} = \begin{cases} S_{ske} & \sigma' < \sigma'_{max} \\ S_{skv} & \sigma' > \sigma'_{max} \end{cases} \quad (2)$$

Where Δb is the change in the thickness of the layer with the starting thickness of b, and S_{sk} is the skeletal specific storage. S_{ske} and S_{skv} are the elastic and inelastic (virgin) skeletal specific storage respectively. For more information about the SUB package the reader is referred to the original reference for the full description of the model [10,11].

5. RESULTS AND DISCUSSIONS

Running the 3D-flow transient model shows that the piezometric head decreases in the upper six layers and increases in the three deepest layers for the period 2007-2016. The major head decline and rise have occurred in the fourth (Ruisbroek-Berg aquifer) and eighth (Wemmel-Lede aquifer and sands of Brussels) layers, respectively. Additionally, the aquitard layers experience very minor fluctuations in piezometric head.

Time series measured by applied PSI on ENVISAT radar data and simulated results from the geomechanical model overlap only from July 1, 2007, to July 1, 2010, the comparison period is thus very short.

Although ENVISAT data for the whole period of 2003–2010 have a negative rate (i.e., subsidence) in the local zone of the model, a very slight uplift at the rate of about 1 mm/year is observed during this 'validation' period (2007-2010).

The top five layers are compacted, according to the results of the geomechanical model, while the deepest four layers show a rebound. The Polder deposits and the Tongeren aquitard layers have the highest and lowest amounts of consolidation, respectively. Additionally, the Bartoon aquitard and the Wemmel-Lede aquifer and sands of Brussels layers had the strongest rebound. The rebound of the last layer during the modeling period is insignificant.

The final cumulative displacement simulated by the geomechanical model during the validation period of three years agrees extremely well with the comparable values derived from the PSI approach. This final cumulative displacement obtained by adding the deformation in all layers during the whole period was computed and compared with the equivalent value obtained from the PSI technique at the location of each of the 18 PSs acquired from applying PSI on ENVISAT radar data (Table 1). The calculated Root Mean Square Error (RMSE) between simulated and observed values is equal to 1.2 mm. The differences between observed and simulated displacements are provided in the Forth column of Table 2. Positive numbers represent uplift, whereas negative values represent subsidence.

PS Number	Cumulative displacement observed by PSI (m)	Cumulative displacement simulated in the model (m)	Difference (m)
1	0.00038	0.00133	-0.00095
2	0.00176	0.00133	0.00043
3	0.00214	0.00129	0.00085
4	0.00248	0.00091	0.00157
5	0.00133	0.00160	-0.00027
6	0.00135	0.00160	-0.00025
7	0.00059	0.00159	-0.00100
8	0.00262	0.00159	0.00103
9	0.00037	0.00159	-0.00122
10	0.00090	0.00144	-0.00054
11	-0.00057	0.00146	-0.00203
12	0.00474	0.00143	0.00331
13	0.00108	0.00146	-0.00038
14	0.00109	0.00147	-0.00037
15	0.00069	0.00163	-0.00094
16	0.00314	0.00163	0.00151
17	0.00032	0.00137	-0.00105
18	0.00249	0.00141	0.00108

Table 2: Cumulative total displacement as observed and simulated during the validation period (2007-2010).

More investigations are still needed as the time evolution of the simulated cumulative displacements is not similar to those measured by PSI. Probably, the numerical results are not reliable at the beginning of the period and more meaningful at the end. The RMSE in mm between the PSI displacement time series and the cumulated displacement calculated by the model is highlighted by different colours for each PS point in Fig. 2. In any case, a reliable comparison needs a longer period of comparison/validation.

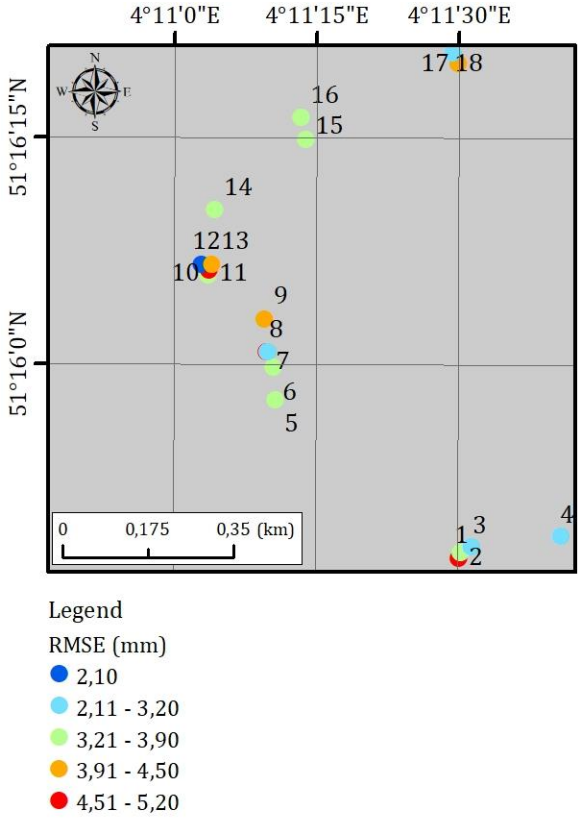

Figure 2: The RMSE (color chart) between the PSI displacement time series and cumulated displacement from the model (during the validation period 2007-2010)

6. CONCLUSION

In this work, a 3D-flow model coupled to a 1D-geomechanical model has been used to assess the main drivers of the displacement that is detected on the surface using the PSI approach. For evaluation of the result, the time series of displacement observed by PSI and simulated by the model are compared over 2007-2010. The amount of total cumulative displacement on the ground surface achieved in the evaluation period using both approaches is fairly in agreement. However, the patterns of the time series produced using the PSI technique and the geomechanical model are not similar. This will be investigated in the future.

11. REFERENCES

[1] Yang, Y., Yang, W., Peng, S., Liu, J., Zhang, T., & Shan, H. (2022). Land deformation monitoring in the Taiyuan area based on PS-InSAR. Environmental Monitoring and Assessment, 194(9), 1-14.

[2] Declercq, P. Y., Gérard, P., Pirard, E., Walstra, J., & Devleeschouwer, X. (2021). Long-term subsidence monitoring of the Alluvial plain of the Scheldt River in Antwerp (Belgium) using radar interferometry. Remote Sensing, 13(6), 1160.

[3] Vandersteen, K., Gedeon, M., & Beerten, K. (2014). A synthesis of hydraulic conductivity measurements of the subsurface in Northeastern Belgium. Geologica Belgica, pp. 61-64.

[4] Yoon, G. L., Kim, B. T., & Jeon, S. S. (2004). Empirical correlations of compression index for marine clay from regression analysis. Canadian Geotechnical Journal, 41(6), 1213-1221.

[5] Dassargues, A. (2018). Hydrogeology: groundwater science and engineering. CRC Press, pp. 158-161.

[6] Report concerning the data of the drilling and the results of the laboratory research carried out for the study of the construction of the 3rd channel dock in the linkerschedt area at left board area at Kallo-kieldrecht-verrebroek and Waasland port of Beveren, Department of Geotechnics, Department of Mobility and Public Works, Belgium

[7] Deng, Y. F., Tang, A. M., Cui, Y. J., Nguyen, X. P., Li, X. L., & Wouters, L. (2011). Laboratory hydro-mechanical characterization of Boom Clay at Essen and Mol. Physics and Chemistry of the Earth, Parts A/B/C, 36(17-18), 1878-1890.

[8] Nguyen, X. P., Yu-Jun Cui, Anh Minh Tang, Xiang Ling Li, and Laurent Wouters. "Physical and microstructural impacts on the hydro-mechanical behavior of Ypresian clays." Applied clay science 102 (2014): 172-185.

[9] Lo, W., Purnomo, S. N., Dewanto, B. G., & Sarah, D. (2022). Integration of numerical models and InSAR techniques to assess land subsidence due to excessive groundwater abstraction in the coastal and lowland regions of Semarang city. Water, 14(2), 201.

[10] Hoffmann, J., Leake, S. A., Galloway, D. L., & Wilson, A. M. (2003). MODFLOW-2000 ground-water model--User guide to the subsidence and aquifer-system compaction (SUB) package. Geological Survey Washington DC, pp. 7-8.

[11] Hoffmann, J. (2003). The application of satellite radar interferometry to the study of land subsidence over developed aquifer systems. Stanford University, pp. 16-19.

ACKNOWLEDGMENT

This research is funded under the Brain BELSPO program called LASUGEO (2019-2023) entitled “monitoring LAnd SUbsidence caused by Groundwater exploitation through gEOdetic measurements”. We wish to thank the European Space Agency (ESA) for providing Envisat ASAR radar data. We also convey our sincere gratitude to Dr. Leen De Vos and Chandra Algoe from the Geotechnics unit at the Department of Mobility and Public Works (MOW) for allowing access to the geotechnical data and to Johan Lhermytte for providing us with hydrogeological parameters.